Nigerian Journal of Neuroscience

https://www.nsn.org.ng/journal/

Original Article

Vanadium Impairs Neuronal Cytoarchitecture of the Hippocampal Trisynaptic Loop in the African Giant Rat (*Cricetomys gambianus*, Waterhouse)

Oluwaseun A. Mustapha[1], Micheal Awala-Ajakaiye[1], Boluwatife Agbalu[1], Stephen T. Bello[2], Matthew A. Olude[1], James O. Olopade[3]

[1]Department of Veterinary Anatomy, College of Veterinary Medicine, Federal University of Agriculture, Abeokuta, Nigeria
[2]Department of Biomedical Sciences, City University of Hong Kong, Kowloon Tong, Kowloon, Hong Kong
[3]Department of Veterinary Anatomy, Faculty of Veterinary Medicine, University of Ibadan, Ibadan, Nigeria

ABSTRACT

Environmental pollution with vanadium may pose neurotoxicity threats to known unique neural attributes (cognition and olfaction) of the African giant rat (AGR). This rodent lives within the same ecological zones as the human populace. Thus, experimental investigations on the effect of vanadium on this rodent may mirror latent epidemiological scenarios in the human populace. This work was designed to evaluate the neurotoxic effect of vanadium on the hippocampal neuronal infrastructure and circuitry and provide cellular correlates to its significant pathologies in the AGR. Twelve adult male AGRs were assigned into two groups (n = 6/group; vanadium and control). They were dosed daily with 3 mg/kg body sodium metavanadate and sterile water for 14 days, respectively, and harvested brains were processed for histology. Using Nissl and Golgi staining techniques with stereological analysis, we demonstrated the effect of vanadium on AGR neuronal architecture of the hippocampal trisynaptic loop as a probable cellular mechanism of vanadium-induced memory deficits. Specifically, the most significant pathologies were seen in the dentate gyrus and CA3, with significantly decreased neuronal density disrupted cytoarchitecture and loss of dendritic arborisations and axonal extensions. At the same time, hippocampal subfields CA2 and CA4 showed region-specific resistance to vanadium-induced neurotoxicity. Furthermore, the selective vulnerability to vanadium-induced neurotoxicity is adduced. This work has demonstrated the neurotoxic effect of vanadium on the hippocampal subfields and circuitry in the AGR and highlighted its probable impact on their translational purposes. This rodent may be a suitable model for evaluating memory pathologies in neurotoxicological studies.

Correspondence: Oluwaseun A. Mustapha, PhD; Neuroscience Unit, Department of Veterinary Anatomy, College of Veterinary Medicine, Federal University of Agriculture, Abeokuta, Nigeria. E-mail: mustaphaoa@funaab.edu.ng; Phone number: +23348035915275; ORCID: 0000-0001-6049-7379

INTRODUCTION

The African giant pouched rat (Cricetomys gambianus) is one of Africa's indigenous rodent whose unique neurobehavioural attributes (olfaction and cognition) have been adapted to remarkable translational benefits in the clearing of landmines and diagnosis of tuberculosis (Mahoney et al. 2012; Olude et al. 2014; Poling et al. 2015). This has earned them nicknames such as HeroRATs and Sniff rats (Carrington 2014). These neural attributes have been linked to the hippocampus – a functional part of the limbic system and one of the oldest phylogenetic parts of the brain (De Quervain et al. 2017; Mustapha et al. 2019a). Furthermore, the significant role of the hippocampus in behavioural and cognitive functions as well as in memory formation and consolidation has been well documented in the literature (Vanderwolf 1992; Riedel et al. 2000). The histological zones of the AGR hippocampus have been described (Mustapha et al. 2019a). Histologically, the hippocampus is composed of the dentate gyrus and hippocampus proper (CA 1 - 4 subfields). Sensory transfers and memory consolidation occur largely along a unidirectional channel of information through its trisynaptic circuitry (Stepan et al. 2015). This trisynaptic circuit, a neural circuit of synaptic transmission

relays in the hippocampus, consists of three noteworthy cell gatherings: granule cells in the dentate gyrus and pyramidal neurons in CA1 and CA3 (Scharfman 2007). The hippocampal transfer is classified according to their cell type and projection fibres and includes these three primary areas within the hippocampus, and thus collectively, they create the trisynaptic loop (Anderson et al. 2014). The primary projection of the hippocampus occurs between the entorhinal cortex and the dentate gyrus, where signals are transmitted from the parahippocampal gyrus to the dentate gyrus through granule cell fibres collectively referred to as the perforant pathway (Ding 2013; Knierim and Neunuebel 2016). The dentate gyrus then synapses on pyramidal cells in CA3 via mossy cell fibres. CA3 then fires to CA1 by means of Schaffer collaterals which synapse in the subiculum and are helped out through the fornix (van Strien et al. 2009; Kohara et al. 2014).

Studies have revealed the hippocampus to be preferentially vulnerable to a wide variety of toxic insults and disease states, with many central nervous disorders manifesting with hippocampal neuronal loss (Zhang et al. 2011; Gattaz et al. 2011; Padurariu et al. 2012). Thus, pathologies leading to the loss of hippocampal neurons, their afferent projections, and synaptic elaborations often lead to persistent impairment in memory and cognitive function. Chief amongst these toxic insults are heavy metal toxicants from environmental pollution, metabolic perturbations and neurodegenerative diseases (Walsh and Emerich 1988; Anand and Dhikav 2012).

One such heavy metal reported to cause varying toxicities to the brain and, indeed, to a variety of biological systems is vanadium (Ladagu et al. 2020). Vanadium is a transition metal that crosses the blood-brain barrier (Fatola et al. 2019) and causes oxidative stress by reactive oxygen species (ROS) generation, lipid peroxidation, demyelination and neuropathologies in nervous tissues (Mustapha et al. 2014, 2019b; Azeez et al. 2016; Folarin et al. 2017; Ohiomokhare et al. 2020; Olaolorun et al. 2021). It is released in high atmospheric concentrations in its gaseous state as vanadium pentoxide, most especially during gas flaring and burning of fossil fuels (Igado et al. 2012; Fortoul et al. 2014). This environmental pollution may thus pose eco-toxicological threats to the AGR and alter the course of their scientific potential (Usende et al. 2018). More importantly, it may, by extension, mirror the epidemiological picture of the effect of environmental pollution on the human populace. Folarin et al. (2016) and Adebiyi et al. (2018) reported memory deficits in Wistar rats exposed to vanadium by evaluating memory performance outcomes using a Morris water maze. However, the cellular basis of these deficits is yet to be fully elucidated. This work is thus designed to evaluate the probable neurotoxic effect of vanadium on the hippocampal neuronal infrastructure and circuitry and also to provide cellular correlates to its notable pathologies in the AGR.

MATERIALS AND METHODS

Animal Handling
A total number of twelve adult male AGRs were obtained from local hunters who had captured these rodents from the wild in Southwest Nigeria. First, a physical examination was conducted on all the AGRs used for this experiment to exclude physical signs of neural deficits and deformities that may interfere with the purpose of the study. Then, they were transferred to and stabilized for 48 h at the Animal House of the Department of Veterinary Anatomy, College of Veterinary Medicine, the Federal University of Agriculture Abeokuta, Ogun State, Nigeria. All experimental procedures followed the criteria laid down by the College of Veterinary Medicine Research Ethics Committee (CREC) of the Federal University of Agriculture Abeokuta (Ethical Approval Reference Number: FUNNAB/COLVET/CREC/007/18).

Experimental Design and Brain Harvest
The animals were randomly assigned into two groups (n=6): Vanadium (treatment) and control (sterile water). AGR in the vanadium group were dosed with sodium metavanadate daily (Sigma-Aldrich®, St. Louis, MO, USA; pH 7.7; 3 mg/kg body weight; intraperitoneally, IP) according to Folarin et al. (2017), while those of the control group were given sterile water, IP. All animals were dosed daily for 14 days after which they were sacrificed. Anaesthesia was achieved by IP injections of 100 mg/kg ketamine (Ketanir®, India) and 10 mg/kg xylazine (Xylazine 20 Inj®, Holland), after which they were perfused with 4% para-formaldehyde transcardially. Their brains were harvested with a pair of bone nippers as prescribed by Olude et al. (2018). Harvested brains were later post-fixed in 4% paraformaldehyde for 48 h and subsequently processed histologically for Nissl (Cresyl violet) and Golgi stains.

Brain Histological Processing
Coronal sections of 5 μm thickness, were made at the temporal lobes (optic chiasma) level for all sections used in this study. In addition, the Nissl stain (for illustrating neuronal soma and nuclei) and rapid Golgi technique (illustrating neurons with their axonal and dendritic projections) were used to explore the hippocampal histomorphology.

Nissl Technique: The brains were cut into 1-2 mm wide sections in the frontal and horizontal planes. These sections were passed through washing, dehydration, clearing, impregnation and embedding in paraffin wax, and 10 μm sections were cut on a sliding microtome. The slides were then deparaffinised in xylene twice for 5 min each and then in equal parts of xylene and absolute alcohol. They were subsequently hydrated in descending grades of alcohol (100%, 90%, 70% and 50%) and immersed in Cresyl violet solution (2.50 g Cresyl violet in 500 mL distilled water) for 7 min, and rinsed in distilled water for a minute. Sections were then dehydrated through ascending grades of alcohol (70% and 95% ethanol + glacial acetic acid until satisfactory differentiation was observed, and 95% and absolute ethanol). Stained slides were then cover-slipped with

dibutylphthalate polystyrene xylene (DPX) mountant (Pilati 2008).

The Rapid Golgi Technique: Brain slices not more than 4 mm thick were cut in horizontal and frontal planes and immersed in osmium-dichromate solution at room temperature (24℃) for seven days. Next, the pieces were transferred into 0.75% aqueous silver nitrate and kept for 24 h in the dark. Then the pieces were placed back into the same osmium-dichromate solution used in the first step, in which they were left for six days. The immersion of the pieces followed this step into silver nitrate solution for 48 h in the dark. Then they were transferred into a new osmium-dichromate solution for five days. Again, the step with silver nitrate was repeated with an increased time solution for three days. The pieces were then dehydrated in absolute alcohol for 5 min and embedded in a soft paraffin matrix by pressing each piece gently into the melted paraffin. 200 μm sections were made on a sliding microtome. The pieces were transferred into absolute alcohol for 15 min, after which the sections were transferred into oil cloves for 15 min (Mustapha et al. 2019a).

Stitching, Photomicrography and Histology: All the sections were mounted on glass slides and examined under the light microscope (Olympus® CX21FS1). Images of twelve fields of each stained tissue section were captured in a clockwise manner and then stitched together to produce a single photomicrograph of each hippocampal segment using AmScope® Digital Camera Software. The observed histopathology in the hippocampus, including the subfields and cytoarchitecture were appropriately described. Golgi-stained images of the hippocampal subfield CA3 were inverted to enhance better contrast with Picassa Software (version 3.9.0; Build 136.04, 0; U.S.A).

Stereological Analysis: Stereological analysis was performed on the hippocampal subfields (CA1, CA2, CA3 and CA4) and dentate gyrus using FIJI Image analysis software (ImageJ 1.52h; Java 1.8.0_66; 64bit NIH, USA). Pyknotic neurons (with signs of injury) were identified and delineated from intact (healthy) neurons based on the following described criteria:
- Cellular oedema: represented by cells with visibly intact nuclei that showed increased cytoplasm/nucleus size ratio compared to adjacent cells.
- Autolysis: anuclear cells or cells exhibiting abnormal nuclear morphology.
- Darkened and small cells: shrunken cells with increased nuclear compactness.
The number of intact and pyknotic neurons were counted over a surface length of 200 μm according to the method of Ribeiro et al. (2017), and were expressed as intact-pyknotic (I-P) ratio for the control and vanadium groups. No differentiation was made on the type of lesion observed. Dentate neuron density (DND) was calculated as the sum of intact and pyknotic neurons in the granule cell layer of the dentate gyrus over a surface length of 200 μm. In contrast, pyramidal neuron density (PND) was calculated as the sum of intact and pyknotic neurons in the pyram-

idal cell layer of subfields CA1, CA2, CA3 and CA4, respectively, over a surface length of 200 μm.

Data Analysis
Counts were reported as mean ± standard error of the mean. Inferential analysis was carried out with a one-way analysis of variance (ANOVA) and Tukey's post hoc test. Differences in the means of intact and pyknotic neurons were analysed using GraphPad Prism Software (version 4.00; GraphPad Software Inc., San Diego, CA, USA). A value of $p < 0.05$ was set to be of statistical significance.

RESULTS

Vanadium induces Mossy Fibre and Dendritic Loss in the Dentate Gyrus
The dentate gyrus of the AGR in the control group had an intact cytoarchitecture, containing oval shaped dentate granule cells stained with Nissl. This is however contrary to what was noticed in the vanadium-dosed group where loss of cytoarchitecture was observed in the granule cell layer (Fig. 1a-b). Golgi stained sections in the vanadium- dosed group revealed a striking loss of axonal extensions (mossy fibres) and dendritic arborisations in the polymorphic and molecular layers of the dentate gyrus respectively. These processes were however intact in aforementioned layers in the control group (Fig. 1c-d). This pathology was further corroborated by a lower DND and a lower I-P ratio in the vanadium group compared to the control (Fig. 1e).

AGR Hippocampal Subfields Showed Selective Vulnerability to Vanadium Toxicity
The cytoarchitecture of the CA1 hippocampal subfield was, to a greater extent, preserved in the vanadium-dosed group (Fig. 2a-b). Although the PND count in CA1 pyramidal cell layer were similar in both the control and vanadium, the I-P ratio was slightly lower in the latter. This was however not statistically significant (p>0.05) (Fig. 2c).
The histology of the subfield CA2 of vanadium-dosed group revealed no striking pathologies and appeared similar to the control group showing intact pyramidal cells with few pyknotic cells (Fig. 3a-b). PND counts and I-P ratio were also consistent with these findings (p>0.05) (Fig. 3c).
Striking neuropathology was however noted in the CA3 pyramidal layer in the vanadium-dosed AGR. There was a significant neuronal loss, large number of pyknotic cells and disruption in the cytoarchitecture of this layer compared to the control (Fig. 4a-b). Golgi stained sections indicated a marked loss of axonal extensions (Schaffer collaterals) and dendritic arborisations of the pyramidal neurons in the vanadium-dosed group as against a more elaborate axonal and dendritic branching in the control (Fig. 4c-d). Apparently intact neurons with higher PND counts were seen in the latter compared to the significantly lower PND counts (p<0.001) recorded in the former (Fig. 4e).

The hippocampal CA4 subfield of the control group had similar histological features with the other CA subfields, with no significant pathology observed. Pyramidal neurons appeared intact with no apparent disruption in cellular integrity and architecture (Fig. 5a-b). No statistical significance was observed in the number of intact and pyknotic cells when both groups were compared (Fig. 5c).

2005; Tashiro et al. 2007; Hainmueller and Bartos 2020). It serves as the first station of synapses in the trisynaptic loop of hippocampal information transfer and memory consolidation via the perforant path of the entorhinal cortex.
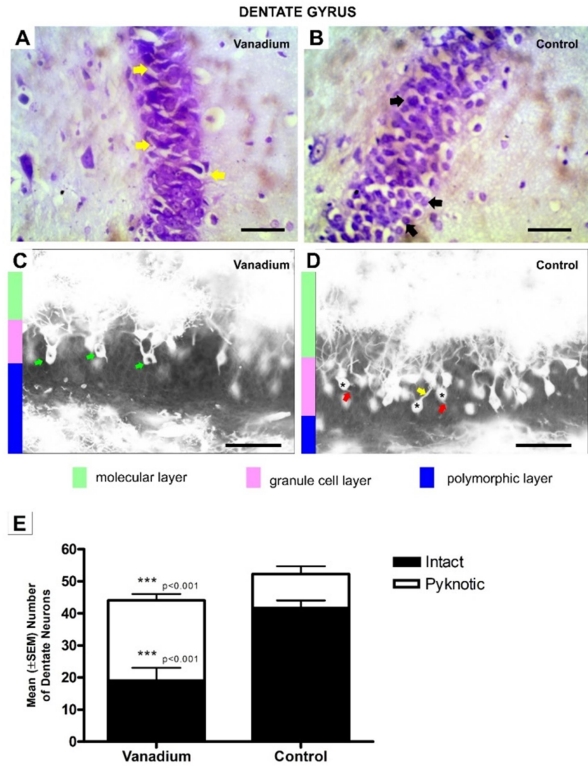

Fig. 1: Dentate gyrus of the AGR. (a and b) Nissl stained sections of vanadium and control groups respectively. Yellow arrows: pyknotic dentate granule cells in the granule cell layer; black arrows: intact dentate granule cells. [c and d]: Golgi stained sections of vanadium and control groups respectively. Green arrows: pyknotic dentate granule cells; asterisks (*): intact dentate granule cells; yellow arrows: intact dendritic arborisations and red arrows: axonal projections [Image inverted]. [e]: Quantitative cell counts of intact and pyknotic dentate granule neurons in the granule cell layer of the dentate gyrus. Scale bars (a-d): 25 µm
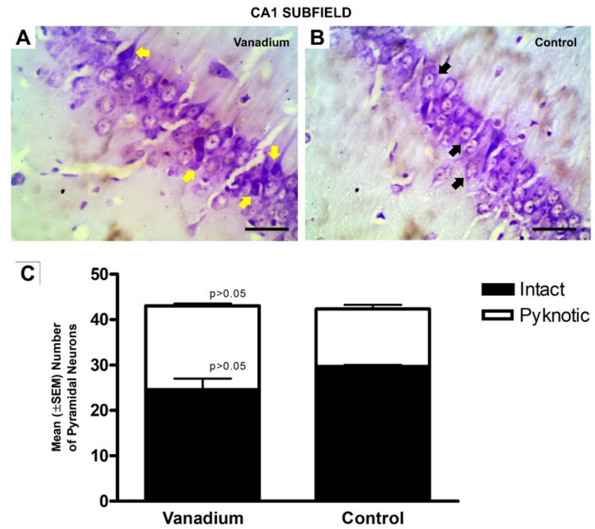

Fig. 2: AGR hippocampal subfield CA1 (a and b) Nissl stained sections of vanadium and control groups respectively. Yellow arrows: pyknotic pyramidal neurons in the pyramidal cell layer; black arrows: intact pyramidal neurons. [c]: Quantitative cell counts of intact and pyknotic pyramidal neurons in the CA1 pyramidal cell layer. Scale bars (a-b): 25 µm
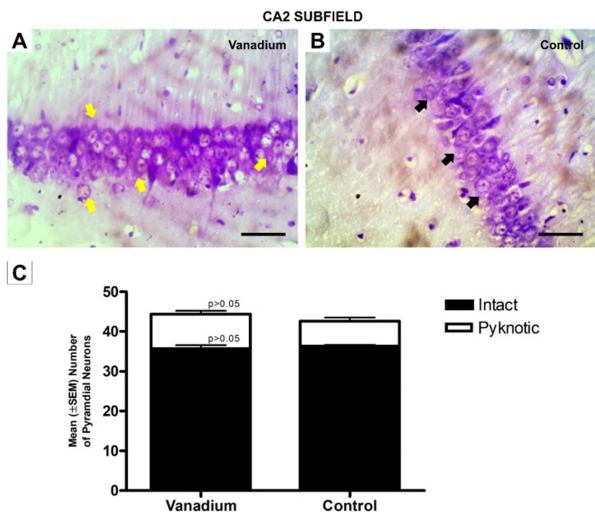

Fig. 3: AGR hippocampal subfield CA2 (a and b) Nissl stained sections of vanadium and control groups respectively. Yellow and black arrows: intact pyramidal neurons. [c]: Quantitative cell counts of intact and pyknotic pyramidal neurons in the CA2 pyramidal cell layer. Scale bars (a-b): 25 µm

DISCUSSION

This study reports the neurotoxic effects of vanadium on hippocampal formation, involving the dentate gyrus and hippocampal proper subfields (CA1-CA4) in the AGR. Using Nissl and Golgi staining techniques with stereological analysis, we demonstrated the effect of vanadium on the neuronal architecture of the hippocampal trisynaptic circuitry (for memory transfer and consolidation) as a probable cellular mechanism of vanadium-induced memory deficits.

The dentate gyrus is a subregion of the hippocampus essential for learning and new memory formation (Li et al.

From our study, a lower I-P granule cell ratio was seen in the dentate gyrus of the vanadium-dosed group. This was

characterized by numerous pyknotic dentate granule cells and a significant reduction in DND, with accompanying loss of dendritic arborisations and disruption in the cytoarchitecture. These neuropathologies are suggestive of a likely interference with the noted function of the dentate gyrus. This notion is further accentuated by the loss of axonal extensions (mossy fibres) of the dentate neurons in the Golgi-stained sections. Mossy fibres transfer information from the dentate gyrus to CA3 pyramidal neurons - the second synaptic unit in the circuit (Scharfman 2007). Dickstein et al. (2007) and Arendt (2009) demonstrated the loss of dendritic arborisations and synapses as one of the earliest changes seen in cognitive disorders.
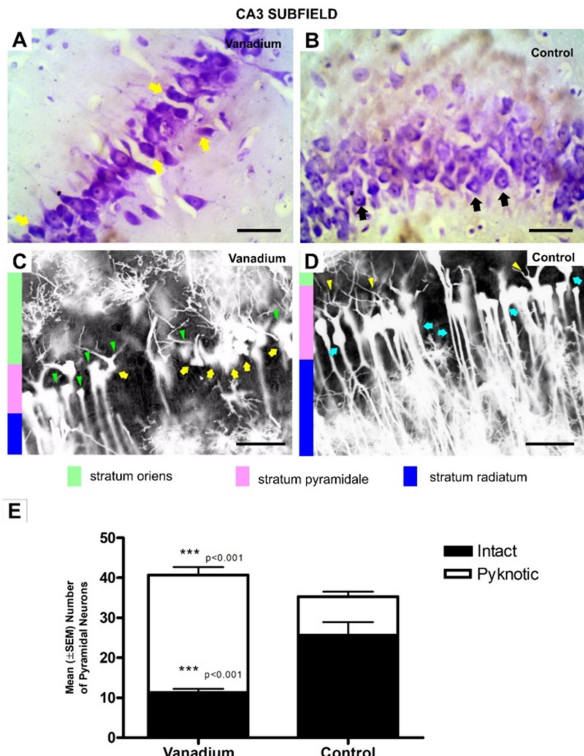

Fig. 4: AGR hippocampal subfield CA3. (a and b): Nissl stained sections of vanadium and control groups respectively. Yellow arrows: pyknotic pyramidal neurons, black arrows: intact pyramidal neurons. [c and d]: Golgi stained sections of vanadium and control groups respectively. green arrowheads: loss of pyknotic pyramidal neurons, yellow arrows: loss of axonal extensions/Schaffer collaterals, red arrows: intact dendritic arborisations and cyan arrows: axonal projections [image inverted]. [e]: Quantitative cell counts of intact and pyknotic pyramidal neurons in the CA3 pyramidal cell layer. Scale bars (a-d): 25 µm

Pyramidal cells of the hippocampal CA1 subfield serve as the major efferent link of the hippocampus to the cortex, either by direct or indirect projection via the subiculum to the cortex (Zierhut et al. 2013). Consequently, pathologies affecting this region of the hippocampus will undoubtedly result in its functional disengagement from these target regions (Harrison and Eastwood 2001). Interestingly, CA1 is particularly noted to be selectively vulnerable to hypoxia and cerebral vascular insults (Harrison and Eastwood 2001; Mattiasson et al. 2003). Our results revealed rela-

tively milder pathologies in the AGR hippocampal CA1 subfield compared to the other subfields, including the control group. This is at variance with reports by Folarin et al. (2017) who noted that hippocampal CA1 pyramidal cells in mice were more susceptible to vanadium-induced cellular degeneration and death. These contrasting findings may possibly result from differences in the formation of ROS and mitochondrial permeability transition pore activation in the CA1 of the AGR compared with other rodents, such as mice and rats (Mattiasson et al. 2003). ROS generated during cellular reduction of vanadate has been implicated in vanadium-induced hypoxia induction factor (HIF)-1α, vascular endothelial growth factor (VEGF) and erythropoietin (EPO) expression via PI3K/AKT/FRAP signalling pathway (Gao et al. 2002; Li et al. 2005; Aschner et al. 2010; Ponce et al. 2013; Fatola et al. 2019). These, via several intermediary signalling, ultimately lead to the inhibition of caspase formation which explains the relatively milder pathologies observed in the AGR hippocampal CA1 subfield.
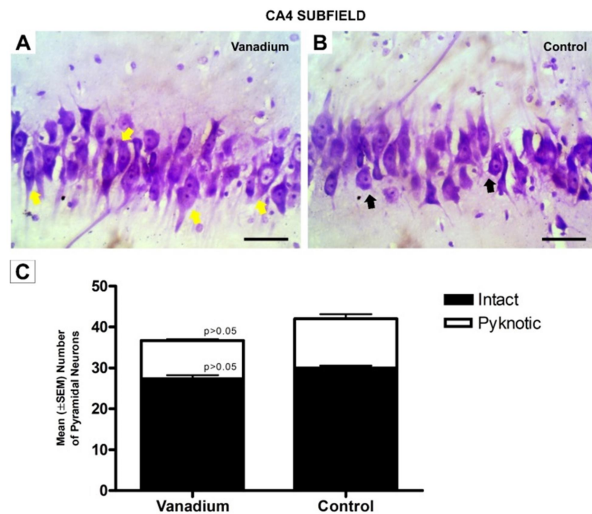

Fig. 5: AGR hippocampal subfield CA4. (a and b): Nissl stained sections of vanadium and control groups respectively. Yellow arrows: pyknotic pyramidal neurons, black arrows: intact pyramidal neurons. [c]: Quantitative cell counts of intact and pyknotic pyramidal neurons in the CA4 pyramidal cell layer. Scale bars (a-b): 25 µm

The CA2 pyramidal neurons are noted to have relatively higher resistance to hypoxia and cell death compared to other CA regions (Maxwell et al. 2003; Steve and Jirsch, 2014; Pang et al. 2019). Simons et al. (2009) suggested a superior calcium-handling capacity of the CA2 pyramidal neurons as accounting for this resistance. The present result agrees, as the CA2 pyramidal neurons revealed no apparent cellular perturbations in the vanadium-dosed AGR, where the I-P ratios and PND were similar to the controls. The most striking neuropathology was observed in the CA3 pyramidal neurons of vanadium-dosed AGR compared to other CA regions, with a noteworthy decrease in neuronal density, alterations in CA3 neuropil, and loss of dendritic arborisations and Schaffer collaterals. This particular subfield region has received a lot of attention for its

specific role in memory processes, and its greater susceptibility to seizures, stress and neurodegeneration (Cherubini and Miles 2015). Vanadate has been demonstrated to generate hydroxyl radicals from superoxide radicals in the presence of nicotinamide adenine dinucleotide hydrogen (NADH) (Shi and Dalal 1993). In fact, the work of Wilde et al. (1997) showed the differential vulnerability of CA1 and CA3 to superoxide and hydroxyl radical, with CA3 showing more hydroxyl radical-mediated damage than CA1. The results from our finding, therefore, suggests that the AGR's hippocampal CA3 NADH drives the generation of hydroxyl radical from vanadate which makes the AGR hippocampal CA3 more susceptible to vanadium-induced damage compared with CA1, and as opposed to previous findings in mice (Folarin et al. 2017). The hydroxyl radical scavenging enzymes in the CA3 of the AGR might have been more compromised following vanadium exposure than those of the CA1, hence the observed neuropathology. The role that chronicity of vanadium exposure has to play in both experiments, however, is left to be proven in the AGR. Moreover, the relative selectivity of CA3 to neuronal damage compared with CA1 following a toxic challenge has also been observed in other studies such as ibotenic acid-induced hippocampal CA3 damage (Conrad et al. 2004) and kainate-induced seizure (Friedman et al. 2003; Liu et al. 2006).

Selective susceptibility of pyramidal neurons to a variety of insults has been reported in the hippocampus (Maxwell et al. 2003), and this may have accounted for the absence of any apparent histopathological observations in the AGR CA4 pyramidal neurons after exposure to vanadium.

As a rule, neuronal and synaptic densities predict the functional capacity of any given brain region or neural structure of interest. More interestingly, previous studies have correlated neuronal losses with memory deficits and cognitive impairments (Korbo et al. 2004; Padurariu 2012). The present study showed neuronal loss, and dendritic and axonal depletions following exposure to vanadium in the AGR. These pathologies may explain the memory deficits recorded in neurobehavioural studies conducted by Folarin et al. (2016) following exposure of Wistar rats to vanadium. More intriguing from our findings is that the cellular gatherings affected by vanadium toxicity (dentate gyrus, CA1 and CA3) represent major stations and pathways in the hippocampal trisynaptic circuitry in new memory formation, transfer and consolidation (Scharfman 2007; Ding 2013).

Factors such as synaptic entry of Ca^{2+} and Zn^{2+} (Medvedeva et al. 2017) and mitochondrial properties (Mattiasson et al. 2003) have been proposed to be involved in the differential vulnerability of the hippocampal CA1 and CA3 regions to toxicants in mice and rats. Our findings further demonstrate that there are possible differences in intra-species hippocampal CA1 and CA3 vulnerability to toxicants; in our case, vanadium in the AGR compared with other rodents.

Conclusion

In conclusion, we demonstrated pathologies in the neuronal architecture of the hippocampal trisynaptic circuitry

exposed to vanadium in the AGR, with the most notable pathologies in the dentate gyrus and CA3. Given the unique neural attributes of the AGR (cognition and strong olfactory prowess) and their translational benefits, as sniff rats where they are deployed in landmine detection and diagnosis of tuberculosis in lung samples, it then becomes expedient to note the impact of environmental pollution (in this case vanadium) on their performance index. Our study also suggests that this indigenous rodent may be a suitable model for evaluating memory pathologies in eco-neurotoxicological researches.

Conflict of Interest
None declared.

Authors' Contribution
Conceptualization: MOA; Data acquisition and Data analysis: MOA, AM, TB; Methodology: MOA, OMA; Resources: MOA, OMA, OJO; Supervision: Olopade JO; Validation: BST, OMA; Visualization and Roles/Writing - Original draft: MOA, AM; Writing – Review & Editing: BST, OMA, OJO. All authors read and approved the final manuscript.

REFERENCES

Adebiyi, O.E., Olopade, J.O. and Olayemi, F.O. (2018) Sodium metavanadate induced cognitive decline, behavioral impairments, oxidative stress and down regulation of myelin basic protein in mice hippocampus: Ameliorative roles of β-spinasterol, and stigmasterol. Brain Behav. 8(7):e01014. https://doi.org/10.1002 /brb3.1014

Anand, K.S. and Dhikav, V. (2012) Hippocampus in health and disease: An overview. Ann Indian Acad Neur. 15(4):239-246. https://doi.org/10.4103/0972-232 7.104323

Anderson, E.B., Grossrubatscher I. and Frank, L. (2014) Dynamic hippocampal circuits support learning- and memory-guided behaviors. Cold Spring Harb Symp Quant Biol. 79:51–58. https://doi.org/10.1101/sqb.2014.79.0247 60

Arendt, T. (2009) Synaptic degeneration in Alzheimer's disease. Acta Neuropathol. 118(1):167-179. https://doi.org/ 10.1007/s00401-009-0536-x.

Aschner, M., Levin, E.D., Sunol, C., Olopade, J.O., Helmcke, K.J., Avila, D.S., et al. (2010) Gene-environment interactions: neurodegeneration in non-mammals and mammals. Neurotoxicology. 31(5):582–588. https://doi.org/ 10.1016/j.neuro.2010.03.008

Azeez, I.A., Olopade, F., Laperchia, C., Andrioli, A., Scambi, I., Onwuka, S.K., et al. (2016) Regional myelin and axon damage and neuroinflammation in the adult mouse brain after long-term postnatal vanadium exposure.

J Neuropathol Exp Neurol. 75(9):843-854. https://doi.org/ 10.1093/jnen/nlw058

Carrington, D. (2014) Hero rats sniff (and snuff) out landmines and TB. http://edition.cnn.com/2014/09/26/ world/africa/hero-rats-sniff-out-landmines-and-tb/

Cherubini, E. and Miles, R. (2015) The CA3 region of the hippocampus: how is it? What is it for? How does it do it? Front Cell Neurosci. 9:19. https://doi.org/10.3389/fncel. 2015.00019

Conrad, C.D., Jackson, J.L. and Wise, L.S. (2004) Chronic stress enhances ibotenic acid-induced damage selectively within the hippocampal CA3 region of male, but not female rats. Neurosci. 125(3):759–767. https://doi.org/10.1016/j. neuroscience.2004.01.049

De Quervain, D., Schwabe, L. and Roozendaal, B. (2017) Stress, glucocorticoids and memory: implications for treating fear-related disorders. Nat Rev Neurosci. 18(1):7–19. https://doi.org/10.1038/nrn.2016.155

Dickstein, D.L., Kabaso, D., Rocher, A.B., Luebke, J.I., Wearne, S.L. and Hof, P.R. (2007) Changes in the structural complexity of the aged brain. Aging Cell. 6(3):275-284. https://doi.org/10.1111/j.1474-9726.2007.00289.x

Ding, S. (2013) Comparative anatomy of the prosubiculum, subiculum, post subiculum, and para subiculum in human, monkey, and rodent. J Comp Neurol 521(18): 4145-4162. https://doi.org/10.1002/cne.23416

Fatola, O.I., Olaolorun, F.A., Olopade, F.E. and Olopade, J.O. (2019) Trends in vanadium neurotoxicity. Brain Res Bull. 145:75-80. https://doi.org/10.1016/j.brainresbull.2018. 03.010

Folarin, O., Olopade, F., Onwuka, S. and Olopade, J. (2016) Memory deficit recovery after chronic vanadium exposure in mice. Oxid Med Cell Longev. 2016: 4860582. https://doi.org/10.1155/2016/4860582

Folarin, O.R., Snyder, A.M., Peters, D.G., Olopade, F., Connor, J.R. and Olopade, J.O. (2017) Brain metal distribution and neuro-inflammatory profiles after chronic vanadium administration and withdrawal in mice. Front Neuroanat. 11:58. https://doi.org/10.3389/fnana.2017.00058

Fortoul, T.I., Rodriguez-Lara, V., González-Villalva, A. Rojas-Lemus, M., Cano-Gutiérrez, G., Ustarroz Cano, M., et al. (2014) Inhalation of vanadium pentoxide and its toxic effects in a mouse model. Inorganica Chimica Acta. 420:8-15. https://doi.org/10.1016/j.ica.2014.03. 027

Friedman, L.K., Velísková, J., Kaur, J., Magrys, B.W. and Liu, H. (2003) GluR2(B) knockdown accelerates CA3 injury after kainate seizures. J Neuropath Exp Neur. 62(7):733-750. https://doi.org/10.1093/jnen/62.7. 733

Gao, N., Ding, M., Zheng, J.Z., Zhang, Z., Leonard, S.S., Liu, K.J., et al. (2002) Vanadate induced expression of hypoxia-inducible factor 1α and vascular endothelial growth factor through phosphati+dylinositol 3-Kinase/Akt pathway and reactive oxygen species, J Biol Chem. 277(35):31963-31971. https://doi.org/10.1074/jbc.M200082 200.

Gattaz, W.F., Valente, K.D., Raposo, N.R., Vincentiis, S. and Talib, L.L. (2011) Increased PLA2 activity in the hippocampus of patients with temporal lobe epilepsy and psychosis. J Psychiatr Res. 45(12):1617-1620. https://doi. org/10.1016/j.jpsychires.2011.07.005

Hainmueller, T. and Bartos, M. (2020) Dentate gyrus circuits for encoding, retrieval and discrimination of episodic memories. Nat Rev Neurosci. 21(3):153–168. https://doi. org/10.1038/s41583-019-0260-z

Harrison, P.J. and Eastwood, S.L. (2001) Neuropathological studies of synaptic connectivity in the hippocampal formation in schizophrenia. Hippocampus. 11(5):508–519. https://doi.org/10.1002/hipo.1067

Igado, O.O., Olopade, J.O., Adesida, A., Aina, O.O. and Farombi, E.O. (2012) Morphological and biochemical investigation into the possible neuroprotective effects of kolaviron (Garcinia kola bioflavonoid) on the brains of rats exposed to vanadium. Drug Chem Toxicol. 35(4):371-380. https://doi.org/10.3109/01480545.2011.630005

Knierim, J.J. and Neunuebel, J.P. (2016) Tracking the flow of hippocampal computation: Pattern separation, pattern completion, and attractor dynamics. Neurobiol Learn Mem. 129:38–49. https://doi.org/10.1016/j.nlm.2015.10.008

Kohara, K., Pignatelli, M., Rivest, A.J., Jung, H.Y., Kitamura, T. and Suh, J. (2014) Cell type-specific genetic and optogenetic tools reveal hippocampal CA2 circuits. Nat Neurosci. 17:269–279. https://doi.org/10.1038/nn.3614

Korbo, L., Amrein, I., Lipp, H.P., Wolfer, D., Regeur, L., Oster, S., et al. (2004) No evidence for loss of hippocampal neurons in non-Alzheimer dementia patients. Acta Neurol Scand. 109:132-139. https://doi.org/10.1034/j.1600-0404.2003.00182.x

Ladagu, A.D., Olopade, F.E., Folarin, O.R., Elufioye, T.O., Wallach, J.V., Dybek, M.B., et al. (2020) Novel NMDA-receptor antagonists ameliorate vanadium neurotoxicity. Naunyn-Schmiedeberg's Arch Pharmacol. 393:1729–1738. https://doi.org/10.1007/s00210-020-01882-6

Li, G. and Pleasure, S.J. (2005) Morphogenesis of the dentate gyrus: what we are learning from mouse mutants. Dev Neurosci 27(2-4):93-99. https://doi.org/10.1159/00008 5980

Li, J., Tong, Q., Shi, X., Costa, M. and Huang, C. (2005) ERKs activation and calcium signaling are both required for VEGF induction by vanadium in mouse epidermal Cl41 cells. Mol Cell Biochem 279(1–2):25–33. https://doi.org/10. 1007/s11010-005-8212-5

Liu, H., Friedman, L.K. and Kaur, J. (2006) Perinatal seizures preferentially protect CA1 neurons from seizure-induced damage in prepubescent rats. Seizure 15(1):1-16. https://doi.org/10.1016/j.seizure.2005.09.0 10

Mahoney, A., Weetjens, B., Cox, C., Beyene, N., Reither, K., Makingi, G., Jubitana, M., Kazwala, R., Mfinanga, G.S., Kahwa, A., Durgin, A. and Poling, A. (2012) Pouched Rats' Detection of Tuberculosis in Human Sputum: Comparison to Culturing and Polymerase Chain Reaction. Tuberc Res and Treat https://doi.org/10.1155/2012/716989

Mattiasson, G., Friberg, H., Hansson, M., Elmér, E. and Wieloch, T. (2003) Flow cytometric analysis of mitochondria from CA1 and CA3 regions of rat hippocampus reveals differences in permeability transition pore activation. J Neurochem 87(2):532-544. https://doi.org/10.1046/j. 1471-4159.2003.02026.x

Maxwell, W.L., Dhillon, K., Harper, L., Espin, J., MacIntosh, T.K., Smith, D.H. and Graham, D.I. (2003) There is differential loss of pyramidal cells from the human hippo-

campus with survival after blunt head injury. J Neuropathol Exp Neurol 62(3):272–279. https://doi.org/10.1093/jnen/62.3.272

Medvedeva, Y.V., Ji, S.G., Yin, H.Z. and Weiss, J.H. (2017) Differential vulnerability of CA1 versus CA3 pyramidal neurons after ischemia: Possible relationship to sources of Zn2+ accumulation and its entry into and prolonged effects on mitochondria. J Neurosci 37:726–737. https://doi.org/10.1523/JNEUROSCI.3270-16.2016

Mustapha, O.A., Oke, B., Offen, N., Sirén, A. and Olopade, J.O. (2014) Neurobehavioral and cytotoxic effects of vanadium during oligodendrocyte maturation: A protective role for erythropoietin. Environ Toxicol Phar 38:98–111. http://dx.doi.org/10.1016/j.etap.2014. 05.001

Mustapha, O.A., Olude, M.A., Bello, S.T., Taiwo, A.I., Jagun, A. and Olopade, J.O. (2019a) Peripheral axonopathy in sciatic nerve of adult wistar rats following exposure to vanadium. J Peripher Nerv Syst. 24:94–99. https://doi.org/10.1111/jns.12294

Mustapha, O.A., Olude, M.A., Taiwo, B. and Olopade, J.O. (2019b) Cytoarchitecture of the hippocampal formation in the African giant rat (Cricetomys gambianus, Waterhouse). Niger J Physiol Sci. 34(1):55-62

Ohiomokhare, S., Olaolorun, F., Ladagu, A., Olopade, F., Howes, M.R., Okello, E., et al. (2020) The pathopharmacological interplay between vanadium and iron in Parkinson's disease models. Int J Mol Sci. 21(18):6719. https://doi.org/10.3390/ijms21186719

Olaolorun, F.A., Olopade, F.E., Usende, L.L., Lijoka, A.D., Ladagu, A.D. and Olopade, J.O. (2021) Neurotoxicity of vanadium. In: Aschner, M. and Costa, L.G. (Eds.) Advances in Neurotoxicology. Massachusetts: Academic Press Elsevier. Pp. 299-327

Olude, M.A., Bello, S.T., Mustapha, O.A., Olopade, F.E., Plendl, J., Ihunwo, A.O., et al. (2018) Oligodendrocyte morphology in the developing brain of the African giant rat (Cricetomys gambianus, Waterhouse): Histology, Immunohistochemistry and Electron microscopy. Anat Histol Embryol. 47(3):231-238. https://doi.org/10.1111/ahe.12348

Olude, M.A., Ogunbunmi, T.K., Olopade, J.O. and Ihunwo, A.O. (2014) The olfactory bulb structure of african giant rat (Cricetomys gambianus, Waterhouse 1840) I: Cytoarchitecture. Anat Sci Int. 89(4):224-231. https://doi.org/10.1007/s12565-014-0227-0

Padurariu, M., Ciobica, A., Mavroudis, L., Fotiou, D. and Baloyannis, S. (2012) Hippocampal neuronal loss in the CA1 and CA3 areas of Alzheimer's disease patients. Psychiat Danub. 24(2):152-158.

Pang, C.C., Kiecker, C., O'Brien, J.T., Noble, W. and Chang, R.C.C. (2019) Ammon's horn 2 (CA2) of the hippocampus: A long-known region with a new potential role in neurodegeneration. Neuroscientist. 25(2):67-180. https://doi.org/10.1177/1073858418778747

Pilati, N., Barker, M., Panteleimonitis, S., Donga, R. and Hamann, M. (2008) A rapid method combining Golgi and Nissl staining to study neuronal morphology and cytoarchitecture. J Histochem Cytochem. 56:539–550. https://doi.org/10.1369/jhc.2008.950246

Poling, A., Mahoney, A., Beyene, N., Mgode, G., Weetjens, B., Cox, C., et al. (2015) Using giant African pouched rats to detect human tuberculosis: A review. Pan Afr Med J. 21:333. https://doi.org/10.11604/pamj.2015.21.333.2977

Ponce, L.L., Navarro, J.C., Ahmed, O. and Robertson, C.S. (2013) Erythropoietin neuroprotection with traumatic brain injury. Pathophysiol. 20(1):31–38. https://doi.org/10.1016/j.pathophys.2012.02.005

Ribeiro, M.C., Bezerra, T.D.S., Soares, A.C., Boechat-Ramos, R., Carneiro, F.P., Vianna, L.M.S., et al. (2017) Hippocampal and cerebellar histological changes and their behavioural repercussions caused by brain ischaemic hypoxia experimentally induced by sodium nitrite. Behav Brain Res. 332:223-232. https://doi.org/10.1016/j.bbr.2017.06.008

Riedel, G., Casabona, G., Platt, B., Macphail, E.M. and Nicoletti, F. (2000) Fear conditioning-induced time and region specific increase in expression of mGlu5 receptor protein in rat hippocampus. Neuropharmacology 39:1943-1951. https://doi.org/10.1016/s0028-3908(00) 00037-x

Scharfman, H.E. (2007) The CA3 "backprojection" to the dentate gyrus. Prog Brain Res. 163:627–637. https://doi.org/10.1016/S0079-6123(07)63034-9

Shi, X. and Dalal, N.S. (1993) Vanadate-mediated hydroxyl radical generation from superoxide radical in the presence of NADH: Haber-Weiss vs Fenton mechanism. Arch Biochem Biophys. 307(2):336-341. https://doi.org/10.1006/abbi.1993.1597

Simons, S.B., Escobedo, Y., Yasuda, R. and Dudek, S.M. (2009) Regional differences in hippocampal calcium handling provide a cellular mechanism for limiting plasticity. Proc Natl Acad Sci. 106 33):14080–14084. https://doi.org/10.1073/pnas.0904775106

Stepan, J., Dine, J. and Eder, M. (2015) Functional optical probing of the hippocampal trisynaptic circuit in vitro: network dynamics, filter properties, and polysynaptic induction of CA1 LTP Front Neurosci. 9. https://doi.org/10.3389/fnins.2015.00160

Steve, T.A., Jirsch, J.D. and Gross, D.W. (2014) Quantification of subfield pathology in hippocampal sclerosis: a systematic review and meta-analysis. Epilepsy Res. 108(8):1279-1285. https://doi.org/10.1016/j.eplepsyres.2014.07.003

Tashiro, A., Makino, H. and Gage, F.H. (2007) Experience-specific functional modification of the dentate gyrus through adult neurogenesis: a critical period during an immature stage. J Neurosci. 27(12):3252-3259. https://doi.org/10.1523/JNEUROSCI.4941-06.2007

Usende, I.L., Alimba, C.G., Emikpe, B.O., Bakare, A.A. and Olopade, J.O. (2018) Intraperitoneal sodium metavanadate exposure induced severe clinicopathological alterations, hepato-renal toxicity and cytogenotoxicity in African giant rats (Cricetomys gambianus, Waterhouse, 1840). Environ Sci Pollut Res Int. 25(26):26383-26393. https://doi.org/10.1007/s11356-018-2588-8

van Strien, N.M., Cappaert, N.L. and Witter, M.P. (2009) The anatomy of memory: an interactive overview of the parahippocampal-hippocampal network. Nat Rev Neurosci. 10:272–282. https://doi.org/10.1038/nrn2614

Vanderwolf, C.H. (1992) Hippocampal activity, olfaction and sniffing: and olfactory input to the dentate gyrus. Brain

Res. 593(2):197-208. https://doi.org/10.1016/0006-8993 (92)91308-2

Walsh, T.J. and Emerich, D.F. (1988) The hippocampus as a common target of neurotoxic agents. Toxicol 49:137-140. https://doi.org/10.1016/0300-483x(88)90185-0

Wilde, G.J., Pringle, A.K., Wright, P. and Iannotti, F. (1997) Differential vulnerability of the CA1 and CA3 subfields of the hippocampus to superoxide and hydroxyl radicals in vitro. J Neurochem. 69(2):883-886. https://doi.org/10.1046/j.1471-4159.1997.69020883.x

Zhang, Z., Liao, W., Chen, H., Mantini, D., Ding, J., Xu, Q., Wang, Z., et al. (2011) Altered functional–structural coupling of large-scale brain networks in idiopathic generalized epilepsy. Brain. 134 (10):12–2928. https://doi.org/10.1093 /brain/awr223

Zierhut, K.C., Graßmann, R., Kaufmann, J., Steiner, J., Bogerts, B. and Schiltz, K. (2013) Hippocampal CA1 deformity is related to symptom severity and antipsychotic dosage in schizophrenia. Brain. 136(3):804-814. https://doi.org/10.1093/brain/aws335.

_____